Soil moisture profile retrievals using reflection of multi-frequency electromagnetic signals

Alexander G. Voronovich and Richard J. Lataitis, *Life Senior Member, IEEE*

***Abstract* - A method for retrieving soil moisture profiles using multi-frequency, ground-reflected electromagnetic waves is considered. In contrast with earlier work, the frequency dependence of the modulus of the reflection coefficient for a single incidence angle is treated in detail. Two possible approaches are considered: the direct retrieval of the soil moisture profile and the retrieval of the dielectric constant profile. The former immediately yields the parameter of interest, however, it requires a numerical model linking the dielectric constant of the soil to its water content. Such a model, which depends on the type of soil, may not be immediately available. The latter does not require a linking model but by comparing measured profiles of the dielectric constant under dry and wet conditions the soil moisture profile can be estimated. Both approaches are considered in this paper and their feasibility is demonstrated with the help of numerical simulations in the presence of multiplicative noise in the data. For the case of a direct retrieval of the soil moisture profile, the Mironov et al. [5] soil model is used. Technical issues associated with the use of a broadband antenna are also discussed**.

***Index Terms* - Soil moisture, remote sensing, reflectometry**

I. INTRODUCTION

The importance of soil moisture (SM) for a variety of key environmental processes is widely acknowledged, and the necessity of accurate measurements of SM hardly requires a justification. It is also broadly recognized that not only surface values of SM but the entire SM profile to at least a meter depth, and optimally up to a few meters depth, is of crucial importance (see, for example, the recent review paper [1]). Measurements of SM by contact sensors is very laborious and are unable to provide significant areal coverage. For this reason, numerous remote sensing techniques were suggested and tested. An overview of the current state of the art in remote sensing of SM can be found in [1,2]. Amongst them, satellite measurements, which provide global coverage, are particularly important. Unfortunately, the relatively high frequencies typically used (most often L-band) do not penetrate deeply into the soil, and the SM retrievals represent integrated values over a depth of approximately 5 cm and horizontal scales on the order of tens of kilometers. P-band signals penetrate deeper into the soil [3], however, a single incidence angle/frequency measurement doesn't provide enough information to accomplish a full SM profile retrieval without employing additional assumptions.

Recently in [2], a method for retrieving SM profiles was proposed based on measurements of the angular and frequency dependence of the modulus of reflection coefficient (i.e., the reflectivity) of meter-to-decameter electromagnetic (EM) waves reflected from the soil. A brief overview of the approach is presented in the next section. The use of relatively low frequencies ensures good penetration of the EM radiation into the soil and, consequently, opens the possibility of inferring not only the surface value of the SM but its depth dependence as well. Numerical experiments performed in [2], which confirmed the feasibility of the method, were based mostly on the angular dependence of the reflectivity at a few discrete frequencies. The retrieval relied on a numerical technique to minimize the difference between a multi-parameter reflectivity model and measured reflectivities. This suggested approach, however, is not easily implemented in practice. An assumption was also made that the dielectric constant of the soil was frequency independent.

In this paper the retrieval technique suggested in [2] is refined and further extended. First, a more realistic model of dielectric properties of the soil (i.e., Mironov *et al.* [5]) is used. Second, the retrieval procedure is simplified, which makes it more robust. Third, instead of considering the angular dependence of the reflectivity, its frequency dependence, which is easier to measure, is examined. Fourth, the assumption of frequency independence of the dielectric constant is removed. Direct SM retrievals require information about the functional relationship between SM and the dielectric constant (DC) of the soil. Such a relationship, although available for certain types of soils, is not necessarily readily available for all locations. An alternative is to retrieve instead the complex DC of the soil before and after a precipitation event, which provides enough information to estimate the SM profile. Unfortunately, because the DC is complex, a relatively high-dimensional parameterization space is still needed for the numerical inversion. Still, we demonstrate that such retrieval is possible, although it requires more involved computer calculations.

The approach outlined in [2] suggested the use of a two small, uncrewed aircraft systems (UASs or drones) to implement the

This paragraph of the first footnote will contain the date on which you submitted your paper for review. It will also contain support information, including sponsor and financial support acknowledgment. For example, "This work was supported in part by the U.S. Department of Commerce under Grant BS123456".

Alexander G. Voronovich is with the NOAA Physical Sciences Laboratory, 325 Broadway, Boulder, CO, 80305. Richard J. Lataitis is with the Science and Technology Corporation, Hampton, VA, 23666 assigned to the NOAA Physical Sciences Laboratory.

technique. The advantage over existing approaches would be the possibility of rapidly mapping SM profiles to one-meter depth with a horizontal resolution on the order of tens of meters. This would fill a critical gap between current in-situ and satellite-based SM measurements that would allow for measurements of the spatial inhomogeneity of the SM field at grid scales that could potentially improve climate model simulations. This approach requires relatively compact and light antennas, which have to be rather broadband. A design of an antenna which satisfies these requirements is also briefly considered.

II. OUTLINE OF THE APPROACH

As noted in [2], the reflectivity of the soil can be measured by mounting an EM transmitter and a receiver on two drones separated by distances on the order of 100 m and operating at heights of a similar scale (e.g., see Fig. 1). For a source located at a point $(0, z_S)$ and a receiver at a point (r, z_R), the total received signal (ψ_{tot}), which is the superposition of a direct (ψ_{dir}) and a surface-reflected (ψ_{ref}) signal, can be expressed as:

$$\psi_{tot} = \psi_{dir} + \psi_{ref} = \psi_{dir}\left(r, z_R - z_S\right) + V(\theta)\psi_{dir}\left(r, z_R + z_S\right), \quad (1)$$

where $V(\theta)$ is the complex reflection coefficient and θ is the incidence angle defined by $tan\,\theta = r/(z_S + z_R)$. The resulting interference pattern depends on the phase difference between the direct and the surface-reflected signals at the receiver. Slight variations of the locations of the source and/or receiver on the order of a wavelength, for which the incidence angle θ will be essentially constant, will exhibit both fully constructive and fully destructive interference in the total field.

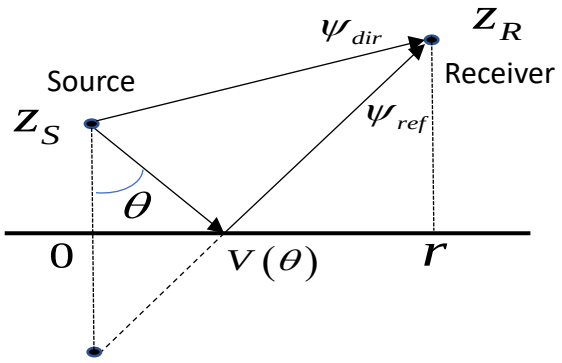

Fig. 1. Illustration of the measurement scheme. A drone-mounted receiving antenna located at a height z_R above the ground plane detects variations in the interference pattern produced by the interaction between the direct Ψ_{dir} and ground-reflected Ψ_{ref} field emanating from a drone-mounted transmitting antenna located above the origin 0 at a height z_S above the ground plane and a distance r from the receiving antenna. $V(\theta)$ is the complex reflection coefficient which varies with the incidence angle θ defined by $tan\,\theta = r/(z_S + z_R)$.

The reflectivity $R = |V(\theta)|$ can then be inferred by calculating ratio of the minimum to maximum values of the total signal:

$$\frac{\left|\psi_{tot}\right|_{min}}{\left|\psi_{tot}\right|_{max}} = \frac{\xi - |V(\theta)|}{\xi + |V(\theta)|}, \quad (2a)$$

where

$$\xi = \left|\frac{\psi_{dir}\left(r, z_R - z_S\right)}{\psi_{dir}\left(r, z_R + z_S\right)}\right|. \quad (2b)$$

Similarly, if the path difference between the direct and surface-reflected wave in Fig. 1 is L, a variation of frequency on the order of Δf:

$$\Delta f \sim \frac{c}{L} \quad (3)$$

will also produce a transition from fully constructive to destructive interference. If $L > 100\ m$, one finds $\Delta f < 3\ MHz$, and within this relatively small frequency bin the variation of reflectivity can be generally neglected. Then, again, (2) can be used to infer the reflectivity through variations of the signal frequency rather than scattering geometry.

Once a set of reflectivity measurements has been obtained, the following Norm can be used to minimize the difference between the modeled and measured reflectivities:

$$Norm = \left(\frac{1}{N_{freq}}\sum_{n=1}^{N_{freq}}\frac{1}{N_{ang}}\sum_{m=1}^{N_{ang}}\left|R\left(f_m, \theta_n\right) - \tilde{R}\left(f_m, \theta_n\right)\right|^{q_1}\right)^{q_2}. \quad (4)$$

Here $R(f_m, \theta_n)$ and $\tilde{R}(f_m, \theta_n)$ are the modeled and measured reflectivities, respectively, which are functions of the EM frequency f and wave incidence angle θ. N_{freq} and N_{ang} are the total number of frequencies and angles used, and the indices q_1 and q_2 are arbitrary parameters that can be chosen to optimize the minimization. The modeled reflectivity $R(f_m, \theta_n)$ depends on the profile of the dielectric constant of the soil, which, in turn, depends on an electrodynamic and geophysical model of the soil. We characterize the electrodynamic model by the complex dielectric constant ε and the geophysical model by a specific SM profile.

In particular, in [2] the following electrodynamic model was employed:

$$\varepsilon = 3 + (56 + 7i)m_v, \quad (5)$$

where m_v is a volumetric measure of the SM. (We note that the soil moisture SM can be represented as the % ratio of volume of water to volume of soil (m_v) or the % ratio of the difference between the mass of moist and dry soil and the mass of the dry soil (m_g)). This approximate relation follows from Fig. 11a of [4]. The depth dependence of m_v (the geophysical model) was represented by the following Gaussian function:

$$m_v = m_v^{(max)} exp\left(-\frac{\left(z - z_{max}\right)^2}{d^2}\right), \quad (6)$$

which depends on the three parameters $(m_v^{(max)}, z_{max}, d)$. The indices of the Norm in (4) were set to $q_1 = q_2 = 2$. The reason for the latter choice was a requirement for the smoothness of the

Norm with respect to the minimization parameters or, more specifically, the continuity of the corresponding second derivatives.

The feasibility of the approach was verified in [2] with the help of numerical simulations. Using the selected electrodynamic and geophysical models, the reflectivities were calculated and then artificially distorted by adding a certain amount of a random noise:

$$\tilde{V} = V(1 + NL \cdot \eta), \tag{7}$$

where η is a random complex number with uncorrelated real and imaginary parts and unit variances:

$$\langle (Re\ \eta)^2 \rangle = \langle (Im\ \eta)^2 \rangle = 1, \quad \langle Re\ \eta \cdot Im\ \eta \rangle = 0, \tag{8}$$

and NL is a real factor that we will be referring to as "noise level". The random complex numbers η are uncorrelated for different frequencies and incidence angles. The resulting reflectivities $R = |V|$ in (4) are considered as "measured".

The Norm minimization procedure in [2] was executed as follows. First, the Norm defined in (4) was calculated for a relatively sparse grid of the 3-dimensional geophysical parameter space, and local minima were determined. Then, starting from those local minima, the minimization of Norm was executed iteratively along certain "principal directions", that is, along the eigenvectors of the corresponding Hessian matrix (a "refined" search). This procedure, although somewhat susceptible to being trapped in local minima (if any), in practice appeared to be rather robust and worked well. The downside was a necessity to be able to analytically calculate the Hessian matrix, which is a laborious procedure. In this paper we will be using more straightforward approach.

III. RETRIEVAL OF THE SOIL MOISTURE PROFILE

The retrieval of SM profiles considered in [2] was based primarily on the angular dependence of the reflectivity (121 incidence angles uniformly distributed within $10^o - 70^o$ interval) at only a few frequencies. In practice, however, it may be more convenient to measure the frequency dependence of the reflectivity at only a few incidence angles since in this case the continuous changing of the geometry of measurements associated with the positioning of the transmitter and receiver in space is not needed. This is the approach explored in this paper, that is, we consider a retrieval based on the frequency dependence of the reflectivity at a single incidence angle. Another difference from [2] is in the selection of different indices for the Norm (4), which in what follows were set to $q_1 = q_2 = 1$.

As far as an electrodynamic model is concerned, the Mironov *et al.* in [5] is employed in this work. This model uses a gravimetric $m_g$rather than volumetric $m_v$measure of SM. Although it has been verified only for a limited set of soil types [6], the physical considerations on which it is based suggest it has a potentially broader applicability. In addition to m_g, this model uses three additional soil-characterization parameters: clay content, temperature, and dry density. The following values (corresponding to a particular sample amongst processed soils) were assumed in this work: clay content = 0.091, temperature = 20^o C, and dry density = 1.575 g/cm^3.

Let us consider first the simplest geophysical model:

$$m_g(z) = m_g^{(0)} + \frac{m_g^{(h)} - m_g^{(0)}}{h} z, \tag{9}$$

which assumes a linear dependence of SM on depth within a layer of thickness h. There are three geophysical parameters in this model: $m_g^{(0)}$ at the surface $z = 0$, $m_g^{(h)}$ at depth h, and the depth h itself. It is assumed that beneath level $z = h$, the SM becomes constant and equal to $m_g^{(h)}$. The model in (9) represents a transition from a moist to drier soil (or vice versa). A single incidence angle is chosen to be $\theta = 45^0$and the frequency varied from 10 MHz to 150 MHz with a 5 MHz step so that $N_{freq} = 29$. The actual values of the geophysical parameters are shown in the second row of Table 1. The depth dependence of both the real and imaginary parts of the complex dielectric constant ε for the lowest and highest frequencies is shown in Fig. 2. The dependencies appear to be close to linear.

TABLE I
ACTUAL AND RETRIEVED PARAMETER VALUES
FOR THE GEOPHYSICAL MODEL IN (9)

Value	$m_g^{(0)}$	$m_g^{(h)}$	$h\,(m)$
Actual	0.1200	0.0600	0.8000
Retrieved	0.1190	0.0541	0.8312

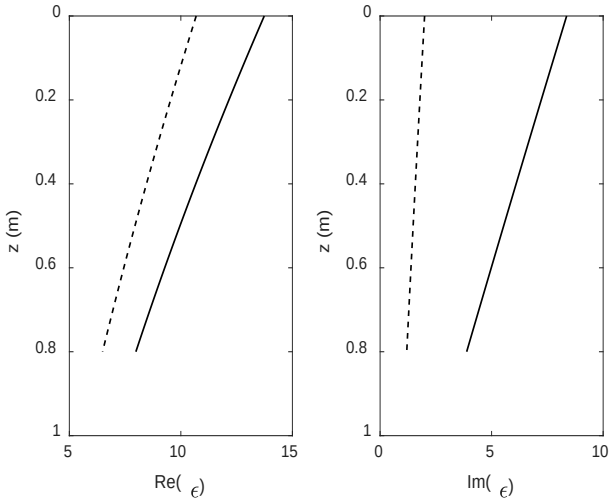

Fig. 2. The simulated depth dependence of the real and imaginary parts of the dielectric constant for 10 MHz (solid lines) and 150 MHz (dashed line) for the geophysical model described in (9).

In Fig. 3 the dependence of the Norm (4) for the moisture profile corresponding to (9) and the actual geophysical parameters listed in the second row of Table 1 is shown. The *k*-th panel, *k = 1,2,3* (counting from the top) corresponds to the situation for which the

k-th geophysical parameter in the set $(m_g^{(0)}, m_g^{(h)}, h)$ varies within certain limits with the other parameters set to exact values. The exact value of the k-th parameter is marked on the x-axis by an asterisk. The upper panels correspond to $q_1 = q_2 = 2$ and the lower panels to $q_1 = q_2 = 1$. One can see that for $q_1 = q_2 = 2$ the minima are much broader than those for $q_1 = q_2 = 1$, which will result in a greater retrieval accuracy for a higher level of noise, but a worse accuracy for a lower level of noise. In what follows we use $q_1 = q_2 = 1$.

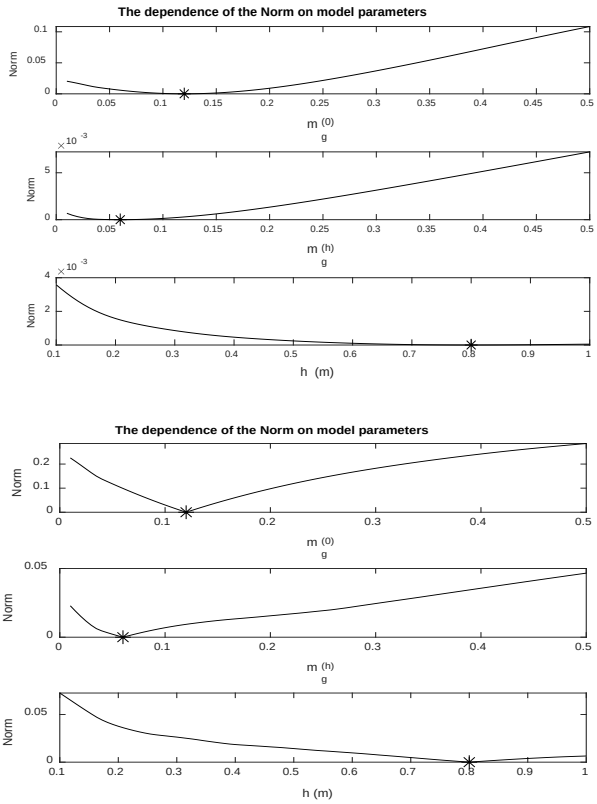

Fig. 3. Dependence of the Norm (4) on the parameter values for the geophysical model described in (9). The upper panels correspond to the case $q_1 = q_2 = 2$ in the calculation of the Norm (4) and the lower panels to $q_1 = q_2 = 1$.

The retrieval was made for vertical polarization and a noise level $NL = 0.01$. The limits of the search were set to:

$$\left(m_g^{(0)}, m_g^{(h)}, h\right)_{min} = (0,\ 0,\ 0.1\ m), \text{ and}$$
$$\left(m_g^{(0)}, m_g^{(h)}, h\right)_{max} = (0.5,\ 0.5,\ 1.0\ m).$$

The parameters $m_g^{(0)}$ and $m_g^{(h)}$ were set to span all realistic SM values. Within the limits of the search 81 points were uniformly distributed across all three parameters, yielding a total of $81^3 = 531,441$ grid points. Four local minima were found within this three-dimensional parameter space and then a search of the absolute minima in the vicinity of each local minimum was executed. The following now deviates from the approach used in [2]. The neighboring cells in the parameter space adjacent to the cell containing a local minimum were linked, with the resulting set of 3^3=27 cells now defining a smaller rectangular search area. Then, within this domain, 11 points were uniformly distributed along all three parameter axes, and an absolute minimum amongst the calculated $11^3 = 1331$ Norms was selected as a final retrieval. The results are shown in Fig. 4. The top panel shows the frequency dependence of the actual (perturbed by noise) and retrieved reflectivities, and the bottom the actual and the retrieved SM profile. The quality of the retrieval is in general very good and becomes exact in the absence of noise.

Note the smooth dependence of the noise with frequency in Fig. 4. The dependence of the reflectivity on frequency is a smooth (analytic) function regardless of the smoothness of the dielectric constant profile. For this reason, random errors in the reflectivity that are uncorrelated for different frequencies can be smoothed before processing. The smoothing procedure was simulated here by including only the first two harmonics of the random noise η as a function of frequency index.

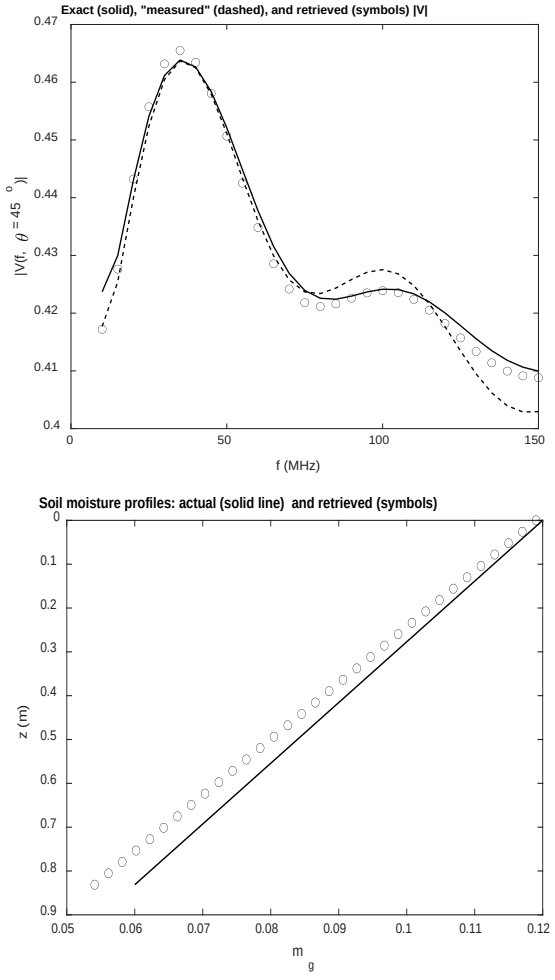

Fig. 4. *Top panel* - The dependence of the reflectivity $|V|$ on frequency for the geophysical model described in (9). An incidence angle of 45° and vertical polarization was assumed. The solid line represents the exact values, the dashed line the "measured" values, and the circles the retrieved values. *Bottom panel* - The actual (sold line) and retrieved (circles) soil moisture profiles.

To generalize the development, in (10) we consider the same SM profile as in the previous example but distorted by adding to it a parabolic term, that is:

$$m_g(z) = m_g^{(0)} + \left(m_g^{(h)} - m_g^{(0)}\right)\left[\frac{z}{h} + c\,\frac{z}{h}\left(1 - \frac{z}{h}\right)\right], \qquad (10)$$

where $c = 0.83$. We applied to this profile the same retrieval procedure as above, that is, finding the parameters $(m_g^{(0)}, m_g^{(h)}, h)$ that minimize the Norm in (4). As a first example, we neglect for the moment the parabolic term in (10) (i.e., $c = 0$) to model the situation for which the SM profile is assumed to be linear in the inversion scheme but actually has a quadratic component. The results are shown in Fig. 5. Clearly there is a mismatch between the actual and retrieved profiles although qualitatively they are in reasonable agreement. In this case we haven't added noise to the data. A separate calculation shows that for $NL = 0.01$ the results change only slightly. This simulation demonstrates the sensitivity of the frequency dependence of the reflectivity to the SM profile, which can be retrieved to reasonable accuracy provided the measurement error is small enough.

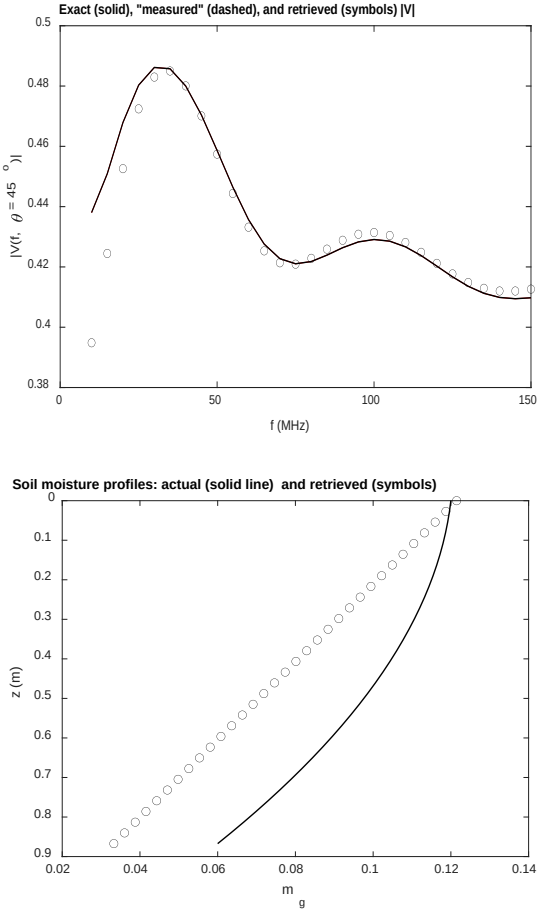

Fig. 5. *Top panel* - The dependence of the reflectivity $|V|$ on frequency for an incidence angle of 45º and vertical polarization. In contrast with Fig. 4 the inversion assumed a linear dependence of the soil moisture profile when it actually included the quadratic component described in (10). The solid line represents the exact values, the dashed line the "measured" values, and the circles the retrieved values. The first two are coincident because the noise level was set to 0. *Bottom panel* - The actual (sold line) and retrieved (circles) soil moisture profiles.

The next example considers the curvature of the SM profile in the inversion. It is convenient to represent the SM profile in this case in slightly different form, namely:

$$m_g(z) = m_g^{(h)}\left(1 + \frac{(z-h)^2}{w_s}\right) \qquad (11)$$

with the set of geophysical parameters to be retrieved being $\left(m_g^{(h)}, h, w_s\right)$.

The actual values of these parameters were set to:

$$\left(m_g^{(h)},\, h,\, w_s\right) = \left(0.06,\, 0.5\ m,\, 1.8\ m^2\right),$$

the noise level to $NL = 0.01$ as before, and the limits of search to:

$$\left(m_g^{(h)},\, h,\, w_s\right)_{min} = \left(0.01,\, 0.3\ m,\, 1.0\ m^2\right), \text{ and}$$
$$\left(m_g^{(h)},\, h,\, w_s\right)_{max} = \left(0.11,\, 0.7\ m,\, 3.0\ m^2\right).$$

The results of the retrieval are shown in Table 2 and Fig. 6. The maximum error of the SM retrieval is approximately 0.004 (< 7%), which is usually considered acceptable.

TABLE II
ACTUAL AND RETRIEVED PARAMETER VALUES
FOR THE GEOPHYSICAL MODEL IN (11)

Value	$m_g^{(h)}$	$h(m)$	$w_s(m^2)$
Actual	0.0600	0.500	1.800
Retrieved	0.0608	0.450	1.45

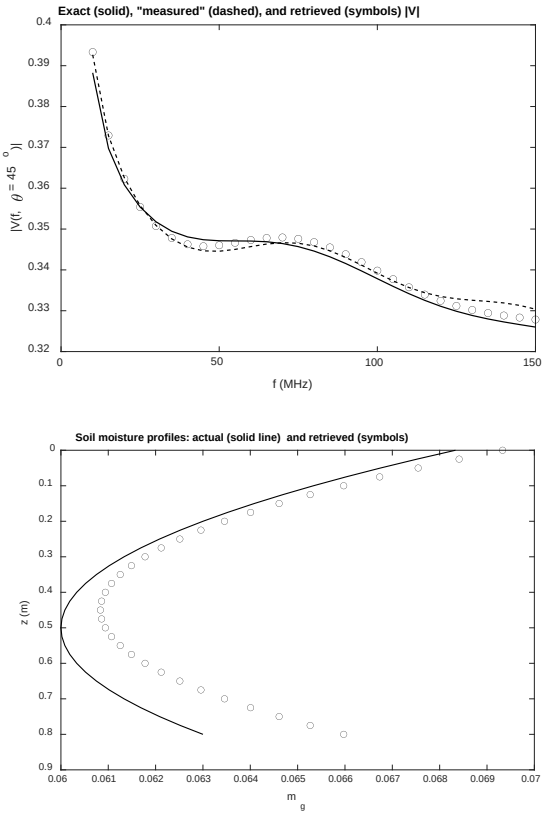

Fig.6. The same as Fig. 4, however, for the soil moisture profile described in (11).

IV. RETRIEVAL OF THE DIELECTRIC CONSTANT PROFILE

Retrievals of soil moisture as presented in the previous section require knowledge of the dependence of the dielectric constant on moisture. Such an approach has the advantage of operating in a parameter space of relatively low dimension equal to the number of parameters in the SM model. However, considering the huge variety of different types of soil, such a model may not be immediately available. For this reason, retrieving a profile of the DC, which is independent of any electrodynamic model, rather than soil moisture itself, may be of interest. If the profiles of the DC can be retrieved at the same location both prior to and after precipitation events, a comparison of the corresponding profiles will provide information about the SM profile. For example, the approximate relations below following from (5) can be used as estimates:

$$\frac{dRe\,\varepsilon}{dm_v} \approx 56, \quad \frac{dIm\,\varepsilon}{dm_v} \approx 7. \tag{12}$$

Retrieval of the DC is an electrodynamic problem that is totally independent of a soil model. The downside of this approach is that a parameter space of much larger dimension is needed for the numerical inversion (generally by a factor of two) because the DC is a complex quantity.

As an example of the retrieval of a DC profile let us consider the following electrodynamic model analogous to the geophysical model given in (10):

$$\varepsilon(z) = \varepsilon^{(0)} + \left(\varepsilon^{(h)} - \varepsilon^{(0)}\right)\left[\frac{z}{h} + c\frac{z}{h}\left(1 - \frac{z}{h}\right)\right], \tag{13}$$

where the six real parameters to be retrieved are:

$$\left(h,\, Re\,\varepsilon^{(0)},\, Im\,\varepsilon^{(0)},\, Re\,\varepsilon^{(h)},\, Im\,\varepsilon^{(h)},\, c\right).$$

Following a similar procedure to that described previously, the actual and retrieved values are shown in Table 3.

TABLE III
ACTUAL AND RETRIEVED PARAMETER VALUES
FOR THE ELECTRODYNAMIC MODEL IN (13)

Value	$h(m)$	$\varepsilon^{(0)}$	$\varepsilon^{(h)}$	c
Actual	1.0	3.00 + 0.10i	14.20 + 1.40i	1.00
Retrieved	0.98	3.56 + 0.16i	11.70 + 1.05i	1.92

The actual values corresponded to (5) with the SM at the top set equal to zero (with a slightly increased imaginary part of $\varepsilon^{(0)}$) and at the bottom set equal to $m_v = 0.2$. As before, vertical polarization was chosen at a single incidence angle of 45° with 29 frequencies uniformly distributed between 10 MHz to 150 MHz with a 5 MHz step. The noise level was set to $NL = 0.05$. Since the number of parameters has now significantly increased to six, the retrieval procedure was somewhat modified. To limit computation time, we used 15 (versus 81) points uniformly distributed across all six parameters, yielding a total of $15^6 = 1{,}139{,}062$ (versus $531,441$) grid points. The search for minima was made iteratively and required several steps. After the first step the local minima found were selected as new starting points, and a new search was initiated over a significantly contracted domain with the same number of 15 points distributed along each of six parameter axes. This process was repeated again and again until the size of the search domain became small enough to resolve the absolute minima. The limits of primary search were set as follows:

$$\left(h, \varepsilon^{(0)}, \varepsilon^{(h)}, c\right)_{min} = (0.8\ m,\ 1.1 + 0i,\ 10 + 1i,\ 0.5),$$
$$\left(h, \varepsilon^{(0)}, \varepsilon^{(h)}, c\right)_{max} = (1.2\ m,\ 5.1 + 0.2i,\ 15 + 2i,\ 1.5),$$

and the entire search now required about 5 hours on a standard PC. The results of the retrieval are shown in Fig. 7.

One can see that the accuracy of the retrieval is reasonable. We note that the information about surface value of the real part of DC is mostly due to the general level of smoothed reflectivity shown in the top panel of the Fig. 7. On the other hand, the depth of the transition level h as well of its general structure is determined by the relatively weak "wavy" component on this figure. Thus, the accuracy of the measurements should be high enough to represent the full profile adequately.

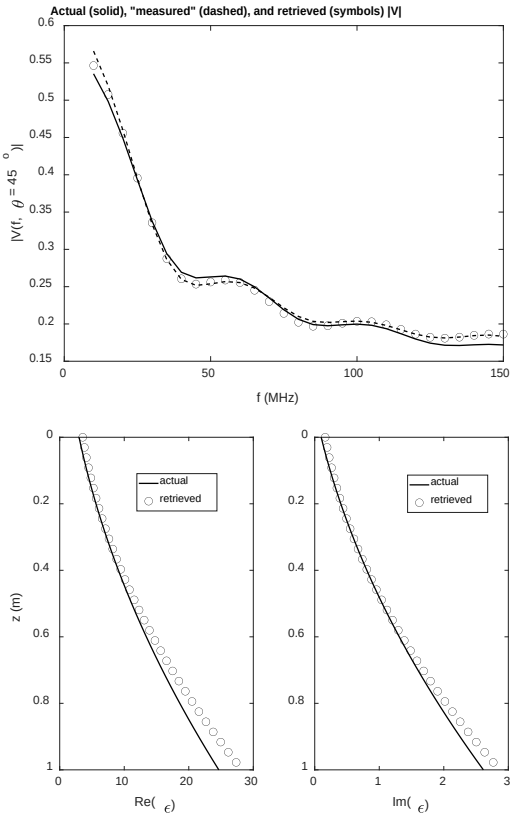

Fig. 7. *Top panel* - The dependence of the reflectivity $|V|$ on frequency for the dielectric constant model described in (13). An incidence angle of 45° and vertical polarization was assumed. The solid line represents the exact values, the dashed line the "measured" values, and the circles the retrieved values. *Bottom panel* - The actual (sold line) and retrieved (circles) dielectric profiles.

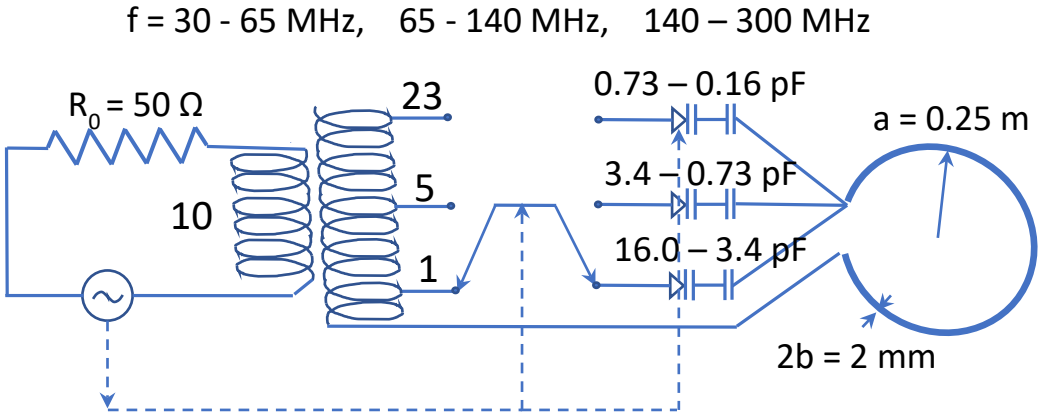

Fig. 8. Proposed design of a broadband circular loop antenna.

V. SOME TECHNICAL ISSUES

As our numerical simulations in the previous section demonstrate, the frequency range of the EM signals needed to adequately retrieve a SM profile is rather broad, with the ratio of the largest to smallest frequency being on the order of 10. Since both the transmitting and receiving antenna are intended to be mounted on drones, they need to be relatively small in size and weight. On the other hand, since the typical distance between the transmitter and receiver is intended to be on the order of hundred meters, and different frequencies can be transmitted sequentially one frequency at a time, the power of the transmitted signal can be made rather low, for example, on the order of tens of milliwatts. Thus, the antennas are not required to be very efficient. Below we demonstrate a possible design of a suitable antenna that operates within frequency range 30 – 300 MHz.

The proposed design shown in Fig. 8 is based on an "external active matching network" approach. We consider a loop of 0.5 m diameter. We divide the required 30 – 300 MHz frequency range into three bins: 30 – 65 MHz, 65 – 140 MHz, and 140 – 300 MHz with frequency intervals that are uniformly spread on a logarithmic scale. A generator on left side of the figure produces a sequence of signals spanning 30 - 300 MHz with frequencies separated by about 100 kHz. The signal then passes through the transformer in the center of the figure. The position of the switch (see below) depends on the bin the current frequency belongs to.

Within each frequency bin, varactors change their capacitance synchronously with change of frequency in inverse proportion to the square of frequency according to (19) below (the circuitry controlling the varactors is not shown). As a result, the inductance of the antenna is always fully compensated and its input impedance becomes real. The ratio of the largest to smallest capacitance of each varactor within the corresponding frequency bin is about 4.6. When the signal varies from one frequency bin to another, the ratio of turns in the transformer also switches from 10:1 for 30 - 65 MHz, to 10:5 for 65 - 140 MHz, and to 10:23 for 140 MHz – 300 MHz.

These ratios are selected so that the resistance of the antenna matches the output resistance of the generator (50 Ω) at the middle frequency of corresponding frequency bin, that is, the generator and the antenna are perfectly matched at 44 MHz, 95 MHz, and 204 MHz. At the terminal frequencies of the bins the resistance of the loop recalculated for the generator circuit become: R_1 = 20 Ω and R_1 = 270 Ω for the first bin, R_1 = 10.8 Ω and R_1 = 247 Ω for the second bin, and R_1 = 11.7 Ω and R_1 = 227 Ω for the third bin.

As a result, the efficiency of the system defined as:

$$eff = \frac{4R_1R_0}{\left(R_1+R_0\right)^2},$$

where R_0 = 50 Ω is the output resistance of the generator, becomes 52 % at worst (when R_1 = 270 Ω). If necessary, the efficiency can be optimized and increased further (note the jump at the resistance R_1 at 65 MHz).

The following relations were used in the above analysis. The impedance of the loop antenna is given by:

$$Z_A = R + j\left(L + L_i\right)\omega, \tag{15}$$

where, according to Eq. (5.24) in [7], the resistance R can be expressed as:

$$R = 20\pi^2\left(\frac{2\pi a}{\lambda}\right)^4 = 20\pi^6\left(\frac{2a}{\lambda}\right)^4, \tag{16}$$

and inductance L as:

$$\begin{aligned} L &= \mu_0 a\left(\log\frac{8a}{b}-2\right)= \\ &= 4\pi\cdot 10^{-7}\cdot 0.25\cdot\left(\log\frac{2}{10^{-3}}-1\right)\approx 1.8\ \mu H. \end{aligned} \tag{17}$$

Here $a = 0.25\ m$ is radius of the loop and $b = 1\ mm$ is radius of the wire. The internal inductance L_i in (15) is given by Eq. (5.38a) in [7]:

$$\begin{aligned} L_i &= \frac{a}{\omega b}\sqrt{\frac{\omega\mu_0}{2\sigma}} = \frac{a}{b}\sqrt{\frac{\mu_0}{2\omega\sigma}} = \frac{0.25}{10^{-3}}\sqrt{\frac{4\pi\cdot 10^{-7}}{2\cdot 2\pi f\cdot\sigma}} = \\ &= 250\sqrt{\frac{10^{-7}}{10^8\cdot 5.9\cdot 10^8}} \approx 3\cdot 10^{-4}\ \mu H \end{aligned} \tag{18}$$

and can be neglected.

To compensate the reactance due to L in (17) the antenna is connected in series with a varactor with the capacitance set to:

$$C = \frac{1}{(2\pi f)^2 L}. \quad (19)$$

The resistance of the antenna will then be real and due to the transformer, will have an effective resistance R_1 recalculated to the generator circuit of:

$$R_1 = \left(\frac{n_2}{n_1}\right)^2 R, \quad (20)$$

where, according to Fig. 7, $n_1 = 10$ and $n_2 = 1, 5, 23$ for the 30–65 MHz, 65–140 MHz, and 140–300 MHz, frequency bins, respectively.

We emphasize that the values quoted in equations (15)-(20) are only rough estimates. For example, for the shortest waves, (16) strictly speaking does not hold, however, the use of more accurate formulas in general would require more complicated calculations that most likely would not change these estimates significantly. Moreover, the equations used to motivate our antenna design are also approximate and are intended only to explore the feasibility of the approach. In fact, more precise values of the varactor and transformer parameters would probably be best determined experimentally.

These estimates show that building broadband antennas with the required parameters is quite feasible. Another important issue is the need for accurate measurement of the directivity patterns. It is clear from (2) that an accurate measurement of the reflectivity depends on the parameter ξ, which, in turn, requires accurate measurements of the directivity patterns of both the transmitter and receiver. Since the antennas will be interacting with drones, what is in fact needed is directivity of the entire antenna-drone system. This directivity can be measured by hovering both drones at a sufficient far-field height and transmitting/receiving signals of varying frequencies and drone orientations.

I. CONCLUSIONS

It was demonstrated that rather accurate measurements of the soil moisture profile for a realistic model of the dielectric constant of moist soil (Mironov's et al. [5]) can be obtained by measuring the frequency dependence of reflectivity within a 10 MHz – 150 MHz frequency band even at a single incidence angle. A simplified procedure for the numerical retrieval of the profile parameters was suggested and verified. In contrast to the technique described in [2], the procedure doesn't require laborious analytical calculations of the second derivatives of the reflectivity with respect to model parameters replacing it instead by more intense brute-force calculations of the reflectivity within a sufficiently dense grid of points in the parameter space.

It was also demonstrated that retrieval of the profile of complex dielectric constant rather than soil moisture was possible. The advantage of this approach is its independence of any electrodynamic model, which may not necessarily be readily available. This procedure, however, requires intense computer calculations due to the higher dimension of the parameter space. If dielectric constant profiles are retrieved at the same location prior and after precipitation events, information about changes in moisture content at different depths can be obtained using empirically known values on $d\varepsilon/dm_v$.

The design of small, light, broadband antenna suitable for mounting on small drones was also briefly considered.

REFERENCES

[1] E. Babaeian, E. , M. Sadeghi, S.B. Jones, C. Montzka, H. Vereecken, and M. Tuller, "Ground, proximal, and satellite remote sensing of soil moisture," *Reviews of Geophysics*, vol. 57, no. 2, pp. 530- 616, March, 2019.

[2] A. G. Voronovich and R. J. Lataitis, "Soil moisture retrieval using reflection coefficients: numerical experiments," *IEEE Transactions on Geoscience and Remote Sensing*, vol. 59, no. 11, pp. 8957-8967, 18 pp., November, 2021.

[3] M. Sadeghi, A. Tabatabaeenejad, M. Tuller, M. Moghaddam and S. B. Jones, "Advancing NASA's AirMOSS P-band radar root zone soil moisture retrieval algorithm via incorporation of Richards' equation," *Remote Sensing*, vol. 9 no.17, December, 2016.

[4] P. Hoekstra P. and A. Delaney A., "Dielectric properties of soils at UHF and microwave frequencies," *Journal of Geophysical Research*, vol. 79, no.11, pp. 1699-1708, April, 1974.

[5] V. L. Mironov, A. Yu. Karavayskiy, Yu. I. Lukin and I. P. Molostov, "A dielectric model of thawed and frozen Arctic coils considering frequency, temperature, texture and dry density," *International Journal of Remote Sensing*, vol. 41, no. 10, pp. 3845-3865, January, 2020.

[6] L. Zhang, Q. Meng, D. Hu, Y. Zhang, S. Yao and X. Chen, "Comparison of different soil dielectric models for microwave soil moisture retrievals," *International Journal of Remote Sensing*, vol. 41, no. 8, pp. 3054-3069, December, 2019.

[7] C. A. Balanis, "*Antenna Theory - Analysis and Design*", 4th ed. Hoboken, New Jersey, John Wiley and Sons, Inc., 2016.